Climate and atmospheric history of the past 420,000 years from the Vostok ice core, Antarctica

J. R. Petit*, J. Jouzel†, D. Raynaud*, N. I. Barkov‡, J.-M. Barnola*, I. Basile*, M. Bender§, J. Chappellaz*, M. Davis‖, G. Delaygue†, M. Delmotte*, V. M. Kotlyakov¶, M. Legrand*, V. Y. Lipenkov‡, C. Lorius*, L. Pépin*, C. Ritz*, E. Saltzman‖ & M. Stievenard†

* *Laboratoire de Glaciologie et Géophysique de l'Environnement, CNRS, BP96, 38402, Saint Martin d'Hères Cedex, France*
† *Laboratoire des Sciences du Climat et de l'Environnement (UMR CEA/CNRS 1572), L'Orme des Merisiers, Bât. 709, CEA Saclay, 91191 Gif-sur-Yvette Cedex, France*
‡ *Arctic and Antarctic Research Institute, Beringa Street 38, 199397, St Petersburg, Russia*
§ *Department of Geosciences, Princeton University, Princeton, New Jersey 08544-1003, USA*
‖ *Rosenstiel School of Marine and Atmospheric Science, University of Miami, 4600 Rickenbacker Causeway, Miami, Florida 33149, USA*
¶ *Institute of Geography, Staromonetny, per 29, 109017, Moscow, Russia*

The recent completion of drilling at Vostok station in East Antarctica has allowed the extension of the ice record of atmospheric composition and climate to the past four glacial–interglacial cycles. The succession of changes through each climate cycle and termination was similar, and atmospheric and climate properties oscillated between stable bounds. Interglacial periods differed in temporal evolution and duration. Atmospheric concentrations of carbon dioxide and methane correlate well with Antarctic air-temperature throughout the record. Present-day atmospheric burdens of these two important greenhouse gases seem to have been unprecedented during the past 420,000 years.

The late Quaternary period (the past one million years) is punctuated by a series of large glacial–interglacial changes with cycles that last about 100,000 years (ref. 1). Glacial–interglacial climate changes are documented by complementary climate records[1,2] largely derived from deep sea sediments, continental deposits of flora, fauna and loess, and ice cores. These studies have documented the wide range of climate variability on Earth. They have shown that much of the variability occurs with periodicities corresponding to that of the precession, obliquity and eccentricity of the Earth's orbit[1,3]. But understanding how the climate system responds to this initial orbital forcing is still an important issue in palaeoclimatology, in particular for the generally strong ~100,000-year (100-kyr) cycle.

Ice cores give access to palaeoclimate series that includes local temperature and precipitation rate, moisture source conditions, wind strength and aerosol fluxes of marine, volcanic, terrestrial, cosmogenic and anthropogenic origin. They are also unique with their entrapped air inclusions in providing direct records of past changes in atmospheric trace-gas composition. The ice-drilling project undertaken in the framework of a long-term collaboration between Russia, the United States and France at the Russian Vostok station in East Antarctica (78° S, 106° E, elevation 3,488 m, mean temperature −55 °C) has already provided a wealth of such information for the past two glacial–interglacial cycles[4–13]. Glacial periods in Antarctica are characterized by much colder temperatures, reduced precipitation and more vigorous large-scale atmospheric circulation. There is a close correlation between Antarctic temperature and atmospheric concentrations of CO_2 and CH_4 (refs 5, 9). This discovery suggests that greenhouse gases are important as amplifiers of the initial orbital forcing and may have significantly contributed to the glacial–interglacial changes[14–16]. The Vostok ice cores were also used to infer an empirical estimate of the sensitivity of global climate to future anthropogenic increases of greenhouse-gas concentrations[15].

The recent completion of the ice-core drilling at Vostok allows us to considerably extend the ice-core record of climate properties at this site. In January 1998, the Vostok project yielded the deepest ice core ever recovered, reaching a depth of 3,623 m (ref. 17). Drilling then stopped ~120 m above the surface of the Vostok lake, a deep subglacial lake which extends below the ice sheet over a large area[18], in order to avoid any risk that drilling fluid would contaminate the lake water. Preliminary data[17] indicated that the Vostok ice-core record extended through four climate cycles, with ice slightly older than 400 kyr at a depth of 3,310 m, thus spanning a period comparable to that covered by numerous oceanic[1] and continental[2] records.

Here we present a series of detailed Vostok records covering this ~400-kyr period. We show that the main features of the more recent Vostok climate cycle resemble those observed in earlier cycles. In particular, we confirm the strong correlation between atmospheric greenhouse-gas concentrations and Antarctic temperature, as well as the strong imprint of obliquity and precession in most of the climate time series. Our records reveal both similarities and differences between the successive interglacial periods. They suggest the lead of Antarctic air temperature, and of atmospheric greenhouse-gas concentrations, with respect to global ice volume and Greenland air-temperature changes during glacial terminations.

The ice record

The data are shown in Figs 1, 2 and 3 (see Supplementary Information for the numerical data). They include the deuterium content of the ice (δD_{ice}, a proxy of local temperature change), the dust content (desert aerosols), the concentration of sodium (marine aerosol), and from the entrapped air the greenhouse gases CO_2 and CH_4, and the $\delta^{18}O$ of O_2 (hereafter $\delta^{18}O_{atm}$) which reflects changes in global ice volume and in the hydrological cycle[19]. (δD and $\delta^{18}O$ are defined in the legends to Figs 1 and 2, respectively.) All these measurements have been performed using methods previously described except for slight modifications (see figure legends).

The detailed record of δD_{ice} (Fig. 1) confirms the main features of the third and fourth climate cycles previously illustrated by the coarse-resolution record[17]. However, a sudden decrease from interglacial-like to glacial-like values, rapidly followed by an abrupt return to interglacial-like values, occurs between 3,320 and 3,330 m.

In addition, a transition from low to high CO_2 and CH_4 values (not shown) occurs at exactly the same depth. In undisturbed ice, the transition in atmospheric composition would be found a few metres lower (due to the difference between the age of the ice and the age of the gas[20]). Also, three volcanic ash layers, just a few centimetres apart but inclined in opposite directions, have been observed—10 m above this δD excursion (3,311 m). Similar inclined layers were observed in the deepest part of the GRIP and GISP2 ice cores from central Greenland, where they are believed to be associated with ice flow disturbances. Vostok climate records are thus probably disturbed below these ash layers, whereas none of the six records show any indication of disturbances above this level. We therefore limit

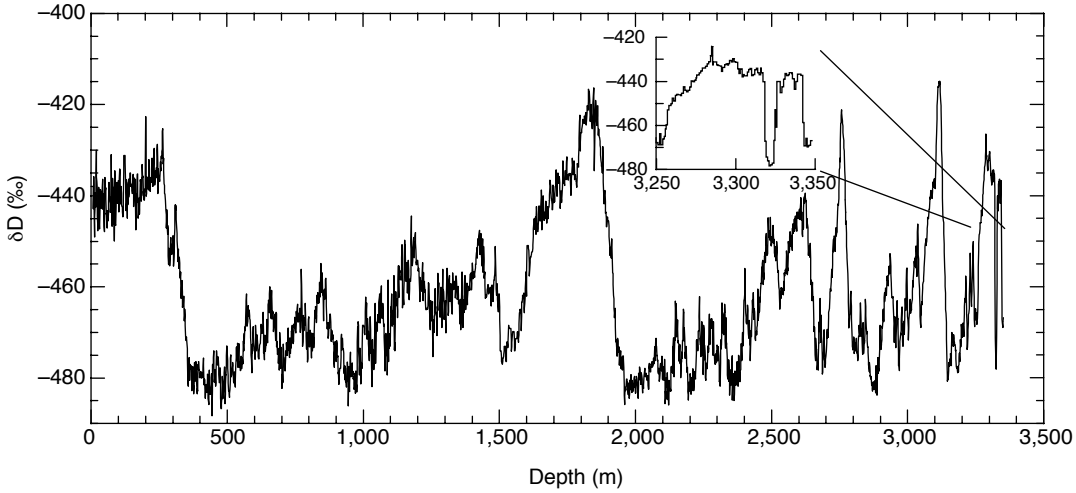

Figure 1 The deuterium record. Deuterium content as a function of depth, expressed as δD (in ‰ with respect to Standard Mean Ocean Water, SMOW). This record combines data available down to 2,755 m (ref. 13) and new measurements performed on core 5G (continuous 1-m ice increments) from 2,755 m to 3,350 m. Measurement accuracy (1σ) is better than 1‰. Inset, the detailed deuterium profile for the lowest part of the record showing a δD excursion between 3,320 and 3,330 m. δD_{ice}(in ‰) = $[(D/H)_{sample}/(D/H)_{SMOW} - 1] \times 1{,}000$.

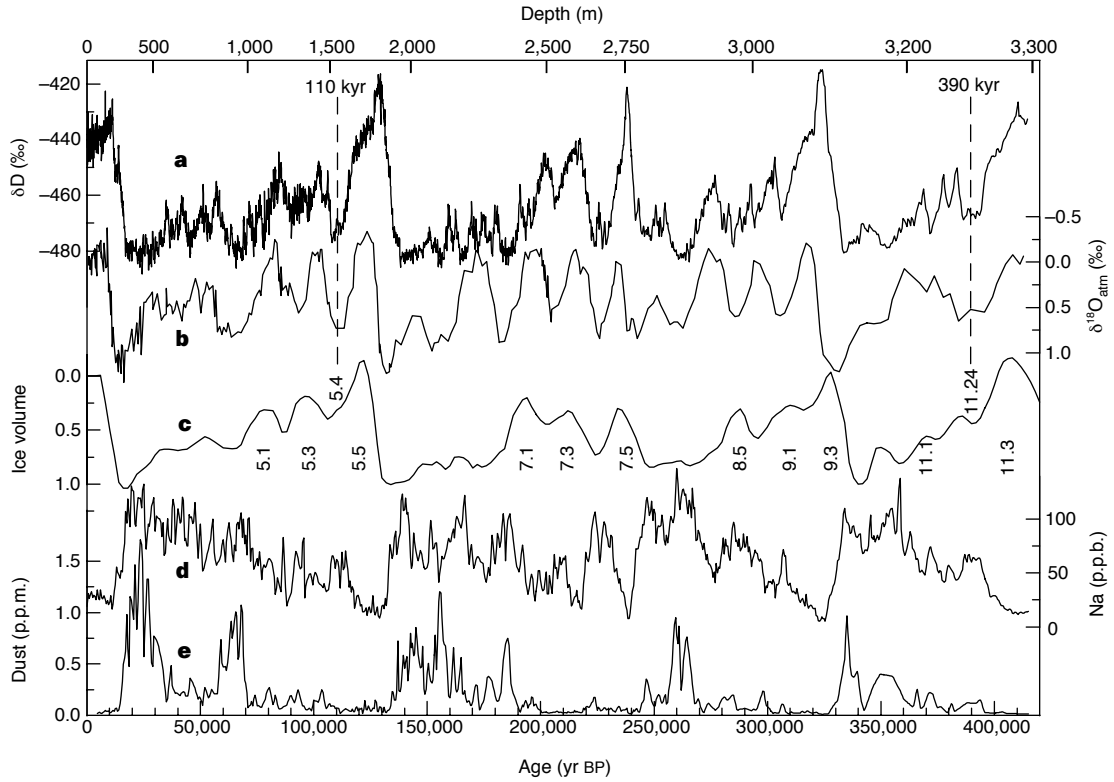

Figure 2 Vostok time series and ice volume. Time series (GT4 timescale for ice on the lower axis, with indication of corresponding depths on the top axis and indication of the two fixed points at 110 and 390 kyr) of: **a**, deuterium profile (from Fig. 1); **b**, $\delta^{18}O_{atm}$ profile obtained combining published data[11,13,30] and 81 new measurements performed below 2,760 m. The age of the gas is calculated as described in ref. 20; **c**, seawater $\delta^{18}O$ (ice volume proxy) and marine isotope stages adapted from Bassinot *et al.*[26]; **d**, sodium profile obtained by combination of published and new measurements (performed both at LGGE and RSMAS) with a mean sampling interval of 3–4 m (ng g^{-1} or p.p.b); and **e**, dust profile (volume of particles measured using a Coulter counter) combining published data[10,13] and extended below 2,760 m, every 4 m on the average (concentrations are expressed in μg g^{-1} or p.p.m. assuming that Antarctic dust has a density of 2,500 kg m^{-3}). $\delta^{18}O_{atm}$(in ‰) = $[(^{18}O/^{16}O)_{sample}/(^{18}O/^{16}O)_{standard} - 1] \times 1{,}000$; standard is modern air composition.

the discussion of our new data sets to the upper 3,310 m of the ice core, that is, down to the interglacial corresponding to marine stage 11.3.

Lorius *et al.*[4] established a glaciological timescale for the first climate cycle of Vostok by combining an ice-flow model and an ice-accumulation model. This model was extended and modified in several studies[12,13]. The glaciological timescale provides a chronology based on physics, which makes no assumption about climate forcings or climate correlation except for one or two adopted control ages. Here, we further extend the Extended Glaciological Timescale (EGT) of Jouzel *et al.*[12] to derive GT4, which we adopt as our primary chronology (see Box 1). GT4 provides an age of 423 kyr at a depth of 3,310 m.

Climate and atmospheric trends

Temperature. As a result of fractionation processes, the isotopic content of snow in East Antarctica (δD or $\delta^{18}O$) is linearly related to the temperature above the inversion level, T_I, where precipitation forms, and also to the surface temperature of the precipitation site, T_S (with $\Delta T_I = 0.67\Delta T_S$, see ref. 6). We calculate temperature changes from the present temperature at the atmospheric level as $\Delta T_I = (\Delta\delta D_{ice} - 8\Delta\delta^{18}O_{sw})/9$, where $\Delta\delta^{18}O_{sw}$ is the globally averaged change from today's value of seawater $\delta^{18}O$, and 9‰ per °C is the spatial isotope/temperature gradient derived from deuterium data in this sector of East Antarctica[21]. We applied the above relationship to calculate ΔT_S. This approach underestimates ΔT_S by a factor of ~2 in Greenland[22] and, possibly, by up to 50% in Antarctica[23]. However, recent model results suggest that any underestimation of temperature changes from this equation is small for Antarctica[24,25].

To calculate ΔT_I from δD, we need to adopt a curve for the change in the isotopic composition of sea water versus time and correlate it with Vostok. We use the stacked $\delta^{18}O_{sw}$ record of Bassinot *et al.*[26], scaled with respect to the V19-30 marine sediment record over their common part that covers the past 340 kyr (ref. 27) (Fig. 2). To avoid distortions in the calculation of ΔT_I linked with dating uncertainties, we correlate the records by performing a peak to peak adjustment between the ice and ocean isotopic records. The $\delta^{18}O_{sw}$ correction corresponds to a maximum ΔT_I correction of ~1 °C and associated uncertainties are therefore small. We do not attempt to correct ΔT_I either for the change of the altitude of the ice sheet or for the origin of the ice upstream of Vostok[13]; these terms are very poorly known and, in any case, are also small (<1 °C).

The overall amplitude of the glacial–interglacial temperature change is ~8 °C for ΔT_I (inversion level) and ~12 °C for ΔT_S, the temperature at the surface (Fig. 3). Broad features of this record are thought to be of large geographical significance (Antarctica and part of the Southern Hemisphere), at least qualitatively. When examined in detail, however, the Vostok record may differ from coastal[28] sites in East Antarctica and perhaps from West Antarctica as well.

Jouzel *et al.*[13] noted that temperature variations estimated from deuterium were similar for the last two glacial periods. The third and fourth climate cycles are of shorter duration than the first two cycles in the Vostok record. The same is true in the deep-sea record, where the third and fourth cycles span four precessional cycles rather than five as for the last two cycles (Fig. 3). Despite this difference, one observes, for all four climate cycles, the same 'sawtooth' sequence of a warm interglacial (stages 11.3, 9.3, 7.5 and 5.5), followed by increasingly colder interstadial events, and ending with a rapid return towards the following interglacial. The

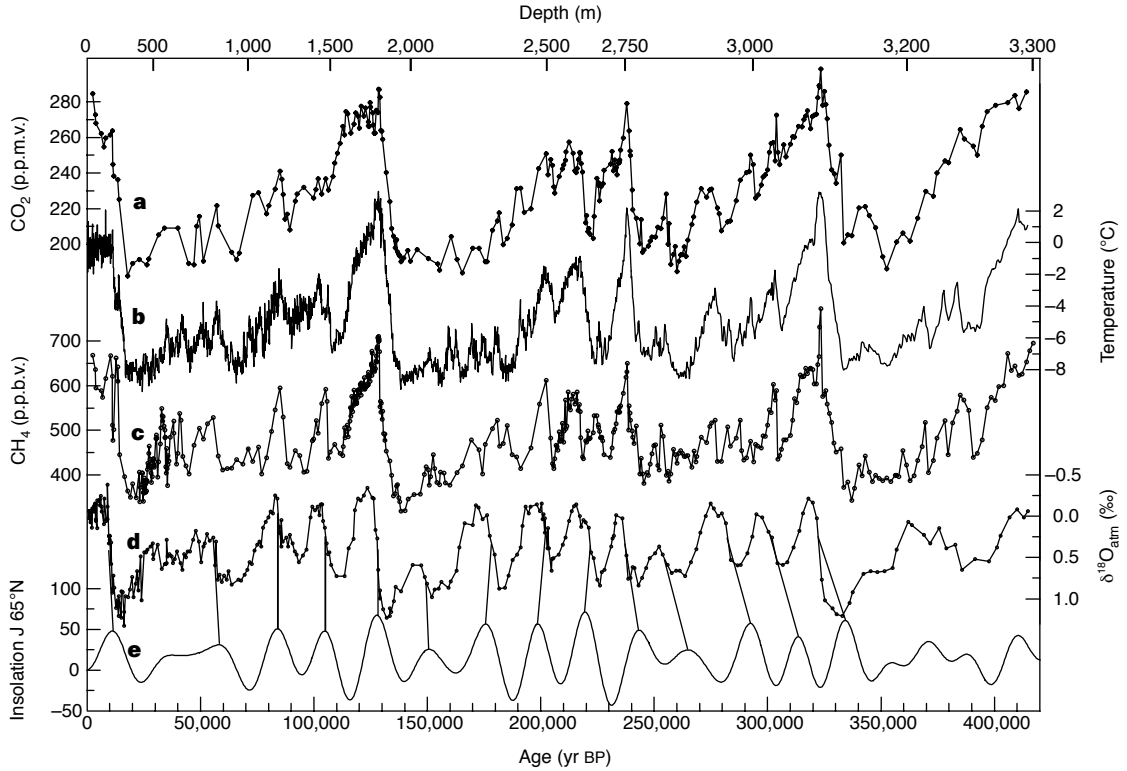

Figure 3 Vostok time series and insolation. Series with respect to time (GT4 timescale for ice on the lower axis, with indication of corresponding depths on the top axis) of: **a**, CO_2; **b**, isotopic temperature of the atmosphere (see text); **c**, CH_4; **d**, $\delta^{18}O_{atm}$; and **e**, mid-June insolation at 65° N (in W m^{-2}) (ref. 3). CO_2 and CH_4 measurements have been performed using the methods and analytical procedures previously described[5,9]. However, the CO_2 measuring system has been slightly modified in order to increase the sensitivity of the CO_2 detection. The thermal conductivity chromatographic detector has been replaced by a flame ionization detector which measures CO_2 after its transformation into CH_4. The mean resolution of the CO_2 (CH_4) profile is about 1,500 (950) years. It goes up to about 6,000 years for CO_2 in the fractured zones and in the bottom part of the record, whereas the CH_4 time resolution ranges between a few tens of years to 4,500 years. The overall accuracy for CH_4 and CO_2 measurements are ±20 p.p.b.v. and 2–3 p.p.m.v., respectively. No gravitational correction has been applied.

coolest part of each glacial period occurs just before the glacial termination, except for the third cycle. This may reflect the fact that the June 65° N insolation minimum preceding this transition (255 kyr ago) has higher insolation than the previous one (280 kyr ago), unlike the three other glacial periods. Nonetheless, minimum temperatures are remarkably similar, within 1 °C, for the four climate cycles. The new data confirm that the warmest temperature at stage 7.5 was slightly warmer than the Holocene[13], and show that stage 9.3 (where the highest deuterium value, –414.8‰, is found) was at least as warm as stage 5.5. That part of stage 11.3, which is present in Vostok, does not correspond to a particularly warm climate as suggested for this period by deep-sea sediment records[29]. As noted above, however, the Vostok records are probably disturbed below 3,310 m, and we may not have sampled the warmest ice of this interglacial. In general, climate cycles are more uniform at Vostok than in deep-sea core records[1]. The climate record makes it unlikely that the West Antarctic ice sheet collapsed during the past 420 kyr (or at least shows a marked insensitivity of the central part of East Antarctica and its climate to such a disintegration).

The power spectrum of ΔT_I (Fig. 4) shows a large concentration of variance (37%) in the 100-kyr band along with a significant concentration (23%) in the obliquity band (peak at 41 kyr). This strong obliquity component is roughly in phase with the annual insolation at the Vostok site[4,6,15]. The variability of annual insolation at 78° S is relatively large, 7% (ref. 3). This supports the notion that annual insolation changes in high southern latitudes influence Vostok temperature[15]. These changes may, in particular, contribute to the initiation of Antarctic warming during major terminations, which (as we show below) herald the start of deglaciation.

There is little variance (11%) in ΔT_I around precessional periodicities (23 and 19 kyr). In this band, the position of the spectral peaks is affected by uncertainties in the timescale. To illustrate this point, we carried out, as a sensitivity test, a spectral analysis using the control points provided by the $\delta^{18}O_{atm}$ record (see Table 1). The position and strength of the 100- and 40-kyr-spectral peaks are unaffected, whereas the power spectrum is significantly modified for periodicities lower than 30 kyr.

Insolation. $\delta^{18}O_{atm}$ strongly depends on climate and related properties, which reflect the direct or indirect influence of insolation[19]. As a result, there is a striking resemblance between $\delta^{18}O_{atm}$ and mid-June insolation at 65° N for the entire Vostok record (Fig. 3). This provides information on the validity of our glaciological timescale

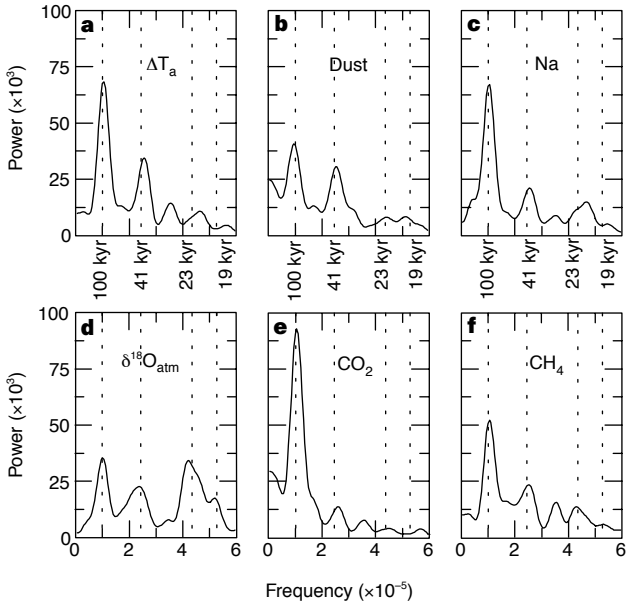

Figure 4 Spectral properties of the Vostok time series. Frequency distribution (in cycles yr^{-1}) of the normalized variance power spectrum (arbitrary units). Spectral analysis was done using the Blackman-Tukey method (calculations were performed with the Analyseries software[47]): **a**, isotopic temperature; **b**, dust; **c**, sodium; **d**, $\delta^{18}O_{atm}$; **e**, CO_2; and **f**, CH_4. Vertical lines correspond to periodicities of 100, 41, 23 and 19 kyr.

Box 1 The Vostok glaciological timescale

We use three basic assumptions[12] to derive our glaciological timescale (GT4); (1) the accumulation rate has in the past varied in proportion to the derivative of the water vapour saturation pressure with respect to temperature at the level where precipitation forms (see section on the isotope temperature record), (2) at any given time the accumulation between Vostok and Dome B (upstream of Vostok) varies linearly with distance along the line connecting those two sites, and (3) the Vostok ice at 1,534 m corresponds to marine stage 5.4 (110 kyr) and ice at 3,254 m corresponds to stage 11.2.4 (390 kyr).

Calculation of the strain-induced thinning of annual layers is now performed accounting for the existence of the subglacial Vostok lake. Indeed, running the ice-flow model[48] with no melting and no basal sliding as done for EGT[12] leads to an age >1,000 kyr for the deepest level we consider here (3,310 m), which is much too old. Instead, we now allow for moderate melting and sliding. These processes diminish thinning for the lower part of the core and provide younger chronologies. We ran this age model[48] over a large range of values of the model parameters (present-day accumulation at Vostok, A, melting rate, M, and fraction of horizontal velocity due to base sliding, S) with this aim of matching the assumed ages at 1,534 and 3,254 m. This goal was first achieved (ages of 110 and 392 kyr) with $A = 1.96\,g\,cm^{-2}\,yr^{-1}$, and M and S equal respectively to $0.4\,mm\,yr^{-1}$ and 0.7 for the region 60 km around Vostok where the base is supposed to reach the melting point (we set $M = 0$ and $S = 0$ elsewhere). These values are in good agreement with observations for A ($2.00 \pm 0.04\,g\,cm^{-2}\,yr^{-1}$ over the past 200 yr) and correspond to a reasonable set of parameters for M and S. We adopt this glaciological timescale (GT4), which gives an age of 423 kyr at 3,310 m, without further tuning (Fig. 2). GT4 never differs by more than 2 kyr from EGT over the last climate cycle and, in qualitative agreement with recent results[49], makes termination I slightly older (by ~700 yr). We note that it provides a reasonable age for stage 7.5 (238 kyr) whereas Jouzel *et al.*[13] had to modify EGT for the second climate cycle by increasing the accumulation by 12% for ages older than 110 kyr. GT4 never differs by more than 4 kyr from the orbitally tuned timescale of Waelbroeck *et al.*[50] (defined back to 225 kyr), which is within the estimated uncertainty of this latter timescale. Overall, we have good arguments[11,50–52] to claim that the accuracy of GT4 should be better than ±5 kyr for the past 110 kyr.

The strong relationship between $\delta^{18}O_{atm}$ and mid-June 65° N insolation changes (see text and Fig. 3) enables us to further evaluate the overall quality of GT4. We can use each well-marked transition from high to low $\delta^{18}O_{atm}$ to define a 'control point' giving an orbitally tuned age. The mid-point of the last $\delta^{18}O_{atm}$ transition (~10 kyr ago) has nearly the same age as the insolation maximum (11 kyr). We assume that this correspondence also holds for earlier insolation maxima. The resulting control points (Fig. 3 and Table 1) are easy to define for the period over which the precessional cycle is well imprinted in 65° N insolation (approximately between 60 and 340 kyr) but not during stages 2 and 10 where insolation changes are small. The agreement between the $\delta^{18}O_{atm}$ control points and GT4 is remarkably good given the simple assumptions of both approaches. This conclusion stands despite the fact that we do not understand controls on $\delta^{18}O_{atm}$ sufficiently well enough to know about the stability of its phase with respect to insolation. We assume that the change in phase does not exceed ±6 kyr (1/4 of a precessional period).

We conclude that accuracy of GT4 is always better than ±15 kyr, better than ±10 kyr for most of the record, and better than ±5 kyr for the last 110 kyr. This timescale is quite adequate for the discussions here which focus on the climatic information contained in the Vostok records themselves.

(see Box 1). The precessional frequencies, which do not account for much variance in ΔT_I, are strongly imprinted in the $\delta^{18}O_{atm}$ record (36% of the variance in this band, Fig. 4). In addition, the remarkable agreement observed back to stage 7.5 between the amplitude of the filtered components of the mid-June insolation at 65° N and $\delta^{18}O_{atm}$ in the precessional band[13] holds true over the last four climate cycles (not shown). As suggested by the high variance of $\delta^{18}O_{atm}$ in the precessional band, this orbital frequency is also reflected in the Dole effect, the difference between $\delta^{18}O_{atm}$ and $\delta^{18}O_{sw}$, confirming results obtained on the last two climate cycles[19,30].

Aerosols. Figure 2 shows records of aerosols of different origins. The sodium record represents mainly sea-salt aerosol entrained from the ocean surface, whereas the dust record corresponds to the small size fraction (~2 μm) of the aerosol produced by the continent. The extension of the Vostok record confirms much higher fallout during cold glacial periods than during interglacials. Concentrations range up to 120 ng g^{-1}, that is, 3 to 4 times the Holocene value, for sea-salt. For dust, they rise from about 50 ng g^{-1} during interglacials to 1,000–2,000 ng g^{-1} during cold stages 2, 4, 6, 8 and 10.

The sodium concentration is closely anti-correlated with isotopic temperature ($r^2 = -0.70$ over the past 420 kyr). The power spectrum of the sodium concentration, like that of ΔT_I, shows periodicities around 100, 40 and 20 kyr (Fig. 4). Conditions prevailing during the present-day austral winter could help explain the observed glacial/interglacial changes in sodium. The seasonal increase of marine aerosol observed in the atmosphere and snow at the South Pole in September[31] corresponds to the maximum extent of sea ice; this is because the more distant source effect is compensated by the greater cyclonic activity, and by the more efficient zonal and meridional atmospheric circulation probably driven by the steeper meridional (ocean–Antarctica) temperature gradient. These modern winter conditions may be an analogue for glacial climates, supporting the apparent close anti-correlation between sodium concentration and temperature at Vostok.

The extension of the Vostok dust record confirms that continental aridity, dust mobilization and transport are more prevalent during glacial climates, as also reflected globally in many dust records (see ref. 10 and references therein). The presence of larger particles in the Vostok record, at least during the Last Glacial Maximum[10], indicates that the atmospheric circulation at high southern latitudes was more turbulent at that time. Lower atmospheric moisture content and reduced hydrological fluxes may also have contributed significantly (that is, one order of magnitude[32]) to the very large increases of dust fallout during full glacial periods because of a lower aerosol-removal efficiency.

Unlike sodium concentration, the dust record is not well correlated with temperature (see below) and shows large concentrations of variance in the 100- and 41-kyr spectral bands (Fig. 4). The Vostok dust record is, in this respect, similar to the tropical Atlantic dust record of de Menocal[33] who attributes these spectral characteristics to the progressive glaciation of the Northern Hemisphere and the greater involvement of the deep ocean circulation. We suggest that there also may be some link between the Vostok dust record and deep ocean circulation through the extension of sea ice in the South Atlantic Ocean, itself thought to be coeval with a reduced deep ocean circulation[34]. Our suggestion is based on the fact that the dust source for the East Antarctic plateau appears to be South America, most likely the Patagonian plain, during all climate states of the past 420 kyr (refs 35, 36). The extension of sea ice in the South Atlantic during glacial times greatly affects South American climate, with a more northerly position of the polar front and the belt of Westerlies pushed northward over the Andes. This should lead, in these mountainous areas, to intense glacial and fluvial erosion, and to colder and drier climate with extensive dust mobilization (as evidenced by glacial loess deposits in Patagonia). Northward extension of sea ice also leads to a steeper meridional temperature gradient and to more efficient poleward transport. Therefore, Vostok dust peaks would correspond to periods of increased sea-ice extent in the South Atlantic Ocean, probably associated with reduced deep ocean circulation (thus explaining observed similarities with the tropical ocean dust record[33]).

Greenhouse gases. The extension of the greenhouse-gas record shows that the main trends of CO_2 and CH_4 concentration changes are similar for each glacial cycle (Fig. 3). Major transitions from the lowest to the highest values are associated with glacial–interglacial transitions. At these times, the atmospheric concentrations of CO_2 rises from 180 to 280–300 p.p.m.v. and that of CH_4 rises from 320–350 to 650–770 p.p.b.v. There are significant differences between the CH_4 concentration change associated with deglaciations. Termination III shows the smallest CH_4 increase, whereas termination IV shows the largest (Fig. 5). Differences in the changes over deglaciations are less significant for CO_2. The decrease of CO_2 to the minimum values of glacial times is slower than its increase towards interglacial levels, confirming the sawtooth record of this property. CH_4 also decreases slowly to its background level, but with a series of superimposed peaks whose amplitude decreases during the course of each glaciation. Each CH_4 peak is itself characterized by rapid increases and slower decreases, but our resolution is currently inadequate to capture the detail of millennial-scale CH_4 variations. During glacial inception, Antarctic temperature and CH_4 concentrations decrease in phase. The CO_2 decrease lags the temperature decrease by several kyr and may be either steep (as at the end of interglacials 5.5 and 7.5) or more regular (at the end of interglacials 9.3 and 11.3). The differences in concentration–time profiles of CO_2 and CH_4 are reflected in the power spectra (Fig. 4). The 100-kyr component dominates both CO_2 and CH_4 records. However, the obliquity and precession components are much stronger for CH_4 than for CO_2.

The extension of the greenhouse-gas record shows that present-day levels of CO_2 and CH_4 (~360 p.p.m.v. and ~1,700 p.p.b.v., respectively) are unprecedented during the past 420 kyr. Pre-industrial Holocene levels (~280 p.p.m.v. and ~650 p.p.b.v., respectively) are found during all interglacials, while values higher than these are found in stages 5.5, 9.3 and 11.3 (this last stage is probably incomplete), with the highest values during stage 9.3 (300 p.p.m.v. and 780 p.p.b.v., respectively).

The overall correlation between our CO_2 and CH_4 records and the Antarctic isotopic temperature[5,9,16] is remarkable ($r^2 = 0.71$ and 0.73 for CO_2 and CH_4, respectively). This high correlation indicates that CO_2 and CH_4 may have contributed to the glacial–interglacial changes over this entire period by amplifying the orbital forcing along with albedo, and possibly other changes[15,16]. We have calculated the direct radiative forcing corresponding to the CO_2, CH_4 and N_2O changes[16]. The largest CO_2 change, which occurs between stages 10 and 9, implies a direct radiative warming of

Table 1 Comparison of the glaciological timescale and orbitally derived information

Depth (m)	Insolation maximum (kyr)	Age GT4 (kyr)	Difference (kyr)
305	11	10	1
900	58	57	1
1,213	84	83	1
1,528	105	105	0
1,863	128	128	0
2,110	151	150	1
2,350	176	179	–3
2,530	199	203	–4
2,683	220	222	–2
2,788	244	239	5
2,863	265	255	10
2,972	293	282	11
3,042	314	301	13
3,119	335	322	13

Control points were derived assuming a correspondence between maximum 65° N mid-June insolation and $\delta^{18}O_{atm}$ mid-transitions. Age GT4 refers to the age of the gas obtained after correction for the gas-age/ice-age differences[20].

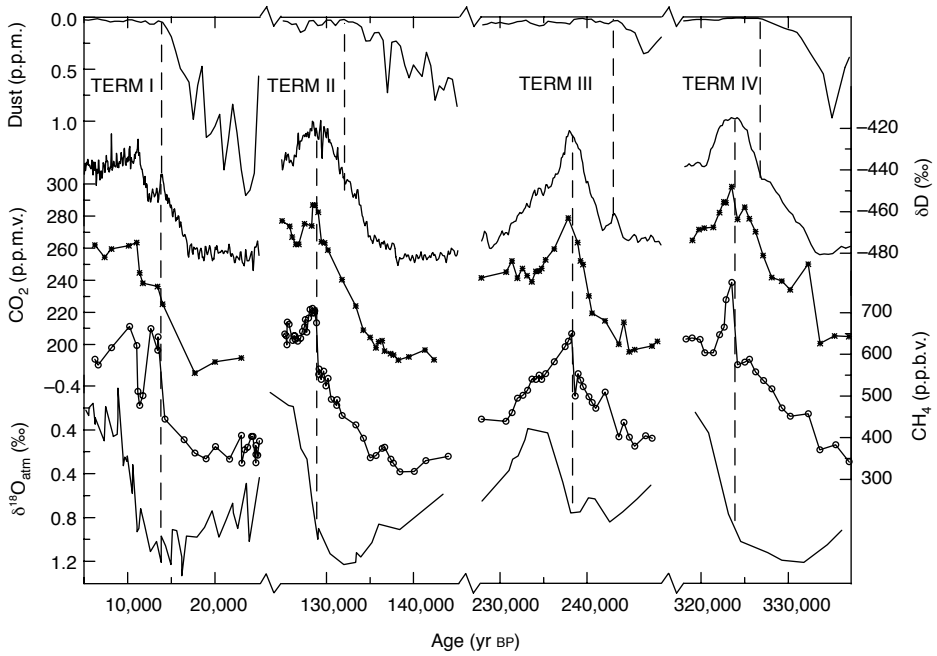

Figure 5 Vostok time series during glacial terminations. Variations with respect to time (GT4) of: **a**, dust; **b**, δD of ice (temperature proxy); **c**, CO_2; **d**, CH_4; and **e**, $\delta^{18}O_{atm}$ for glacial terminations I to IV and the subsequent interglacial periods (Holocene, stage 5.5, stage 7.5 and stage 9.3).

$\Delta T_{rad} = 0.75\,°C$. Adding the effects of CH_4 and N_2O at this termination increases the forcing to 0.95 °C (here we assume that N_2O varies with climate as during termination I[37]). This initial forcing is amplified by positive feedbacks associated with water vapour, sea ice, and possibly clouds (although in a different way for a 'doubled CO_2' situation than for a glacial climate[38]). The total glacial–interglacial forcing is important ($\sim 3\,W\,m^{-2}$), representing 80% of that corresponding to the difference between a 'doubled CO_2' world and modern CO_2 climate. Results from various climate simulations[39,40] make it reasonable to assume that greenhouse gases have, at a global scale, contributed significantly (possibly about half, that is, 2–3 °C) to the globally averaged glacial–interglacial temperature change.

Glacial terminations and interglacials

Our complete Vostok data set allows us to examine all glacial commencements and terminations of the past 420 kyr. We can examine the time course of the following five properties during these events: δD_{ice}, dust content, $\delta^{18}O_{atm}$, CO_2 and CH_4 (Fig. 5). We consider that, during the terminations, $\delta^{18}O_{atm}$ tracks $\delta^{18}O_{sw}$ with a lag of ~2 kyr (ref. 11), the response time of the atmosphere to changes in $\delta^{18}O_{sw}$. $\delta^{18}O_{atm}$ can thus be taken as an indicator of the large ice-volume changes associated with the deglaciations. Broecker and Henderson[41] recently supported this interpretation for the last two terminations and discussed its limitations. Our extended $\delta^{18}O_{atm}$ record indeed reinforces such an interpretation, as it shows that the amplitudes of $\delta^{18}O_{atm}$ changes parallel $\delta^{18}O_{sw}$ changes for all four terminations. $\delta^{18}O_{sw}$ changes are similar for terminations I, II and IV (1.1–1.2‰) but much smaller for termination III (~0.6‰). The same is true for $\delta^{18}O_{atm}$ (1.4–1.5‰ for I, II and IV, and 0.8‰ for III).

A striking feature of the Vostok deuterium record is that the Holocene, which has already lasted 11 kyr, is, by far, the longest stable warm period recorded in Antarctica during the past 420 kyr (Fig. 5). Interglacials 5.5 and 9.3 are different from the Holocene, but similar to each other in duration, shape and amplitude. During each of these two events, there is a warm period of ~4 kyr followed by a relatively rapid cooling and then a slower temperature decrease (Fig. 5), rather like some North Atlantic deep-sea core records[42]. Stage 7.5 is different in all respects, with a slightly colder maximum, a more spiky shape, and a much shorter duration (7 kyr at mid-transition compared with 17 and 20 kyr for stages 5.5 and 9.3, respectively). This difference between stage 7.5 and stages 5.5 or 9.3 may result from the different configuration of the Earth's orbit (in particular concerning the phase of precession with respect to obliquity[3]). Termination III is also peculiar as far as terrestrial aerosol fallout is concerned. Terminations I, II and IV are marked by a large decrease in dust; high glacial values drop to low interglacial values by the mid-point of the δD_{ice} increase. But for termination III, the dust concentration decreases much earlier, with low interglacial values obtained just before a slight cooling event, as for termination I (for which interglacial values are reached just before the 'Antarctic Cold Reversal').

Unlike termination I, other terminations show, with our present resolution, no clear temperature anomalies equivalent to the Antarctic Cold Reversal[6] (except possibly at the very beginning of termination III). There are also no older counterparts to the Younger Dryas CH_4 minimum[43]) during terminations II, III and IV given the present resolution of the CH_4 record (which is no better than 1,000–2,000 yr before stage 5).

The sequence of events during terminations III and IV is the same as that previously observed for terminations I and II. Vostok temperature, CO_2 and CH_4 increase in phase during terminations. Uncertainty in the phasing comes mainly from the sampling frequency and the ubiquitous uncertainty in gas-age/ice-age differences (which are well over ±1 kyr during glaciations and terminations). In a recent paper, Fischer *et al.*[44] present a CO_2 record, from Vostok core, spanning the past three glacial terminations. They conclude that CO_2 concentration increases lagged Antarctic warmings by 600 ± 400 years. However, considering the large gas-age/ice-age uncertainty (1,000 years, or even more if we consider the accumulation-rate uncertainty), we feel that it is premature to infer the sign of the phase relationship between CO_2 and temperature at the start of terminations. We also note that their discussion relates to early deglacial changes, not the entire transitions.

An intriguing aspect of the deglacial CH_4 curves is that the atmospheric concentration of CH_4 rises slowly, then jumps to a maximum value during the last half of the deglacial temperature rise. For termination I, the CH_4 jump corresponds to a rapid Northern Hemisphere warming (Bölling/Allerød) and an increase

in the rate of Northern Hemisphere deglaciation (meltwater pulse IA)[43]. We speculate that the same is true for terminations II, III and IV. Supportive evidence comes from the $\delta^{18}O_{atm}$ curves. During each termination, $\delta^{18}O_{atm}$ begins falling rapidly, signalling intense deglaciation, within 1 kyr of the CH_4 jump. The lag of deglaciation and Northern Hemisphere warming with respect to Vostok temperature warming is apparently greater during terminations II and IV (~9 kyr) than during terminations I and III (~4–6 kyr). The changes in northern summer insolation maxima are higher during terminations II and IV, whereas the preceding southern summer insolation maxima are higher during terminations I and III. We speculate that variability in phasing from one termination to the next reflects differences in insolation curves[41] or patterns of abyssal circulation during glacial maximum. Our results suggest that the same sequence of climate forcings occurred during each termination: orbital forcing (possibly through local insolation changes, but this is speculative as we have poor absolute dating) followed by two strong amplifiers, with greenhouse gases acting first, and then deglaciation enhancement via ice-albedo feedback. The end of the deglaciation is then characterized by a clear CO_2 maximum for terminations II, III and IV, while this feature is less marked for the Holocene.

Comparison of CO_2 atmospheric concentration changes with variations of other properties illuminates oceanic processes influencing glacial–interglacial CO_2 changes. As already noted for terminations I and II[41], the sequence of climate events described above rules out the possibility that rising sea level induces the CO_2 increase at the beginning of terminations. On the other hand, the small CO_2 variations associated with Heinrich events[45] suggest that the formation of North Atlantic Deep Water does not have a large effect on CO_2 concentrations. Our record shows similar relative amplitudes of atmospheric CO_2 and Vostok temperature changes for the four terminations. Also, values of both CO_2 and temperature are significantly higher during stage 7.5 than during stages 7.1 and 7.3, whereas the deep-sea core ice volume record exhibits similar levels for these three stages. These similarities between changes in atmospheric CO_2 and Antarctic temperature suggest that the oceanic area around Antarctica plays a role in the long-term CO_2 change. An influence of high southern latitudes is also suggested by the comparison with the dust profile, which exhibits a maximum during the periods of lowest CO_2. The link between dust and CO_2 variations could be through the atmospheric input of iron[46]. Alternatively, we suggest a link through deep ocean circulation and sea ice extent in the Southern Ocean, both of which play a role in ocean CO_2 ventilation and, as suggested above, in the dust input over East Antarctica.

New constraints on past climate change

As judged from Vostok records, climate has almost always been in a state of change during the past 420 kyr but within stable bounds (that is, there are maximum and minimum values of climate properties between which climate oscillates). Significant features of the most recent glacial–interglacial cycle are observed in earlier cycles. Spectral analysis emphasises the dominance of the 100-kyr cycle for all six data series except $\delta^{18}O_{atm}$ and a strong imprint of 40- and/or 20-kyr periodicities despite the fact that the glaciological dating is tuned by fitting only two control points in the 100-kyr band.

Properties change in the following sequence during each of the last four glacial terminations, as recorded in Vostok. First, the temperature and atmospheric concentrations of CO_2 and CH_4 rise steadily, whereas the dust input decreases. During the last half of the temperature rise, there is a rapid increase in CH_4. This event coincides with the start of the $\delta^{18}O_{atm}$ decrease. We believe that the rapid CH_4 rise also signifies warming in Greenland, and that the deglacial $\delta^{18}O_{atm}$ decrease records rapid melting of the Northern Hemisphere ice sheets. These results suggest that the same sequence of climate forcing operated during each termination: orbital forcing (with a possible contribution of local insolation changes) followed by two strong amplifiers, greenhouse gases acting first, then deglaciation and ice-albedo feedback. Our data suggest a significant role of the Southern Ocean in regulating the long-term changes of atmospheric CO_2.

The Antarctic temperature was warmer, and atmospheric CO_2 and CH_4 concentrations were higher, during interglacials 5.5 and 9.3 than during the Holocene and interglacial 7.5. The temporal evolution and duration of stages 5.5 and 9.3 are indeed remarkably similar for all properties recorded in Vostok ice and entrapped gases. As judged from the Vostok record, the long, stable Holocene is a unique feature of climate during the past 420 kyr, with possibly profound implications for evolution and the development of civilizations. Finally, CO_2 and CH_4 concentrations are strongly correlated with Antarctic temperatures; this is because, overall, our results support the idea that greenhouse gases have contributed significantly to the glacial–interglacial change. This correlation, together with the uniquely elevated concentrations of these gases today, is of relevance with respect to the continuing debate on the future of Earth's climate.

Received 20 January; accepted 14 April 1999.

1. Imbrie, J. *et al.* On the structure and origin of major glaciation cycles. 1. Linear responses to Milankovich forcing. *Paleoceanography* **7,** 701–738 (1992).
2. Tzedakis, P. C. *et al.* Comparison of terrestrial and marine records of changing climate of the last 500,000 years. *Earth Planet. Sci. Lett.* **150,** 171–176 (1997).
3. Berger, A. L. Long-term variations of daily insolation and Quaternary climatic change. *J. Atmos. Sci.* **35,** 2362–2367 (1978).
4. Lorius, C. *et al.* A 150,000-year climatic record from Antarctic ice. *Nature* **316,** 591–596 (1985).
5. Barnola, J. M., Raynaud, D., Korotkevich, Y. S. & Lorius, C. Vostok ice cores provides 160,000-year record of atmospheric CO_2. *Nature* **329,** 408–414 (1987).
6. Jouzel, J. *et al.* Vostok ice core: a continuous isotope temperature record over the last climatic cycle (160,000 years). *Nature* **329,** 402–408 (1987).
7. Raisbeck, G. M. *et al.* Evidence for two intervals of enhanced ^{10}Be deposition in Antarctic ice during the last glacial period. *Nature* **326,** 273–277 (1987).
8. Legrand, M., Lorius, C., Barkov, N. I. & Petrov, V. N. Vostok (Antarctic ice core): atmospheric chemistry changes over the last climatic cycle (160,000 years). *Atmos. Environ.* **22,** 317–331 (1988).
9. Chappellaz, J., Barnola, J.-M., Raynaud, D., Korotkevich, Y. S. & Lorius, C. Ice-core record of atmospheric methane over the past 160,000 years. *Nature* **127–131** (1990).
10. Petit, J. R. *et al.* Paleoclimatological implications of the Vostok core dust record. *Nature* **343,** 56–58 (1990).
11. Sowers, T. *et al.* 135 000 year Vostok—SPECMAP common temporal framework. *Paleoceanography* **8,** 737–766 (1993).
12. Jouzel, J. *et al.* Extending the Vostok ice-core record of palaeoclimate to the penultimate glacial period. *Nature* **364,** 407–412 (1993).
13. Jouzel, J. *et al.* Climatic interpretation of the recently extended Vostok ice records. *Clim. Dyn.* **12,** 513–521 (1996).
14. Genthon, C. *et al.* Vostok ice core: climatic response to CO_2 and orbital forcing changes over the last climatic cycle. *Nature* **329,** 414–418 (1987).
15. Lorius, C., Jouzel, J., Raynaud, D., Hansen, J. & Le Treut, H. Greenhouse warming, climate sensitivity and ice core data. *Nature* **347,** 139–145 (1990).
16. Raynaud, D. *et al.* The ice record of greenhouse gases. *Science* **259,** 926–934 (1993).
17. Petit, J. R. *et al.* Four climatic cycles in Vostok ice core. *Nature* **387,** 359–360 (1997).
18. Kapitza, A. P., Ridley, J. K., Robin, G. d. Q., Siegert, M. J. & Zotikov, I. A. A large deep freshwater lake beneath the ice of central East Antarctica. *Nature* **381,** 684–686 (1996).
19. Bender, M., Sowers, T. & Labeyrie, L. D. The Dole effect and its variation during the last 130,000 years as measured in the Vostok core. *Glob. Biogeochem. Cycles* **8,** 363–376 (1994).
20. Barnola, J. M., Pimienta, P., Raynaud, D. & Korotkevich, Y. S. CO_2 climate relationship as deduced from the Vostok ice core: a re-examination based on new measurements and on a re-evaluation of the air dating. *Tellus B* **43,** 83–91 (1991).
21. Lorius, C. & Merlivat, L. in *Isotopes and Impurities in Snow and Ice. Proc. the Grenoble Symp. Aug./Sept. 1975* 127–137 (Publ. 118, IAHS, 1977).
22. Dahl-Jensen, D. *et al.* Past temperatures directly from the Greenland ice sheet. *Science* **282,** 268–271 (1998).
23. Salamatin, A. N. *et al.* Ice core age dating and paleothermometer calibration on the basis of isotopes and temperature profiles from deep boreholes at Vostok station (East Antarctica). *J. Geophys. Res.* **103,** 8963–8977 (1998).
24. Krinner, G., Genthon, C. & Jouzel, J. GCM analysis of local influences on ice core δ signals. *Geophys. Res. Lett.* **24,** 2825–2828 (1997).
25. Hoffmann, G., Masson, V. & Jouzel, J. Stable water isotopes in atmospheric general circulation models. *Hydrol. Processes* (in the press).
26. Bassinot, F. C. *et al.* The astronomical theory of climate and the age of the Brunhes-Matuyama magnetic reversal. *Earth Planet. Sci. Lett.* **126,** 91–108 (1994).
27. Shackleton, N. J., Imbrie, J. & Hall, M. A. Oxygen and carbon isotope record of East Pacific core V19-30: implications for the formation of deep water in the late Pleistocene North Atlantic. *Earth Planet. Sci. Lett.* **65,** 233–244 (1983).
28. Steig,E. *et al.* Synchronous climate changes in Antarctica and the North Atlantic. *Science* **282,** 92–95 (1998).
29. Howard, W. A warm future in the past. *Nature* **388,** 418–419 (1997).
30. Malaizé, B., Paillard, D., Jouzel, J. & Raynaud, D. The Dole effect over the last two glacial-interglacial cycles. *J. Geophys. Res.* (in the press).
31. Legrand, M. & Delmas, R. J. Formation of HCl in the Antarctic atmosphere. *J. Geophys. Res.* **93,** 7153–7168 (1987).
32. Yung, Y. K., Lee, T., Chung-Ho & Shieh, Y. T. Dust: diagnostic of the hydrological cycle during the last glacial maximum. *Science* **271,** 962–963 (1996).

33. de Menocal, P. Plio-Pleistocene African climate. *Science* **270,** 53–59 (1995).
34. CLIMAP. *Seasonal Reconstructions of the Earth's Surface at the Last Glacial Maximum* (Geol. Soc. Am., Boulder, Colorado, 1981).
35. Basile, I. *et al.* Patagonian origin dust deposited in East Antarctica (Vostok and Dome C) during glacial stages 2, 4 and 6. *Earth Planet. Sci. Lett.* **146,** 573–589 (1997).
36. Basile, I. *Origine des Aérosols Volcaniques et Continentaux de la Carotte de Glace de Vostok (Antarctique)*. Thesis, Univ. Joseph Fourier, Grenoble (1997).
37. Leuenberger, M. & Siegenthaler, U. Ice-age atmospheric concentration of nitrous oxide from an Antarctic ice core. *Nature* **360,** 449–451 (1992).
38. Ramstein, G., Serafini-Le Treut, Y., Le Treut, H., Forichon, M. & Joussaume, S. Cloud processes associated with past and future climate changes. *Clim. Dyn.* **14,** 233–247 (1998).
39. Berger, A., Loutre, M. F. & Gallée, H. Sensitivity of the LLN climate model to the astronomical and CO_2 forcings over the last 200 ky. *Clim. Dyn.* **14,** 615–629 (1998).
40. Weaver, A. J., Eby, M., Fanning, A. F. & Wilbe, E. C. Simulated influence of carbon dioxide, orbital forcing and ice sheets on the climate of the Last Glacial Maximum. *Nature* **394,** 847–853 (1998).
41. Broecker, W. S. & Henderson, G. M. The sequence of events surrounding termination II and their implications for the causes of glacial interglacial CO_2 changes. *Paleoceanography* **13,** 352–364 (1998).
42. Cortijo, E. *et al.* Eemian cooling in the Norwegian Sea and North Atlantic ocean preceding ice-sheet growth. *Nature* **372,** 446–449 (1994).
43. Chappellaz, J. *et al.* Synchronous changes in atmospheric CH_4 and Greenland climate between 40 and 8 kyr BP. *Nature* **366,** 443–445 (1993).
44. Fischer, H., Wahlen, M., Smith, J., Mastroianni, D. & Deck, B. Ice core records of atmospheric CO_2 around the last three glacial terminations. *Science* **283,** 1712–1714 (1999).
45. Stauffer, B. *et al.* Atmospheric CO_2 concentration and millenial-scale climate change during the last glacial period. *Nature* **392,** 59–61 (1998).
46. Martin, J. H. Glacial-interglacial CO_2 change: The iron hypothesis. *Paleoceanography* **5,** 1–13 (1990).
47. Paillard, D., Labeyrie, L. & Yiou, P. Macintosh program performs time-series analysis. *Eos* **77,** 379 (1996).
48. Ritz, C. *Un Modele Thermo-mécanique d'évolution Pour le Bassin Glaciaire Antarctique Vostok-Glacier Byrd: Sensibilité aux Valeurs de Paramètres Mal Connus* Thesis, Univ. Grenoble (1992).
49. Blunier, T. *et al.* Timing of the Antarctic Cold Reversal and the atmospheric CO_2 increase with respect to the Younger Dryas event. *Geophys. Res. Lett.* **24,** 2683–2686 (1997).
50. Waelbroeck, C. *et al.* A comparison of the Vostok ice deuterium record and series from Southern Ocean core MD 88-770 over the last two glacial-interglacial cycles. *Clim. Dyn.* **12,** 113–123 (1995).
51. Blunier, T. *et al.* Asynchrony of Antarctic and Greenland climate change during the last glacial period. *Nature* **394,** 739–743 (1998).
52. Bender, M., Malaizé, B., Orchado, J., Sowers, T. & Jouzel, J. High precision correlations of Greenland and Antarctic ice core records over the last 100 kyr. in *The Role of High and Low Latitudes in Millennial Scale Global Change* (eds Clark, P. & Webb, R.) (AGU Monogr., Am. Geophys. Union, in the press).

Supplementary information is available on *Nature*'s World-Wide Web site (http://www.nature.com) or as paper copy from the London editorial office of *Nature*.

Acknowledgements. This work is part of a joint project between Russia, France and USA. We thank the drillers from the St Petersburg Mining Institute; the Russian, French and US participants for field work and ice sampling; and the Russian Antarctic Expeditions (RAE), the Institut Français de Recherches et Technologies Polaires (IFRTP) and the Division of Polar Programs (NSF) for the logistic support. The project is supported in Russia by the Russian Ministry of Sciences, in France by PNEDC (Programme National d'Études de la Dynamique du Climat), by Fondation de France and by the CEC (Commission of European Communities) Environment Programme, and in the US by the NSF Science Foundation.

Correspondence and requests for materials should be addressed to J.R.P. (e-mail: petit@glaciog.ujf-grenoble.fr).